Below are Supplementary Figures 1-10

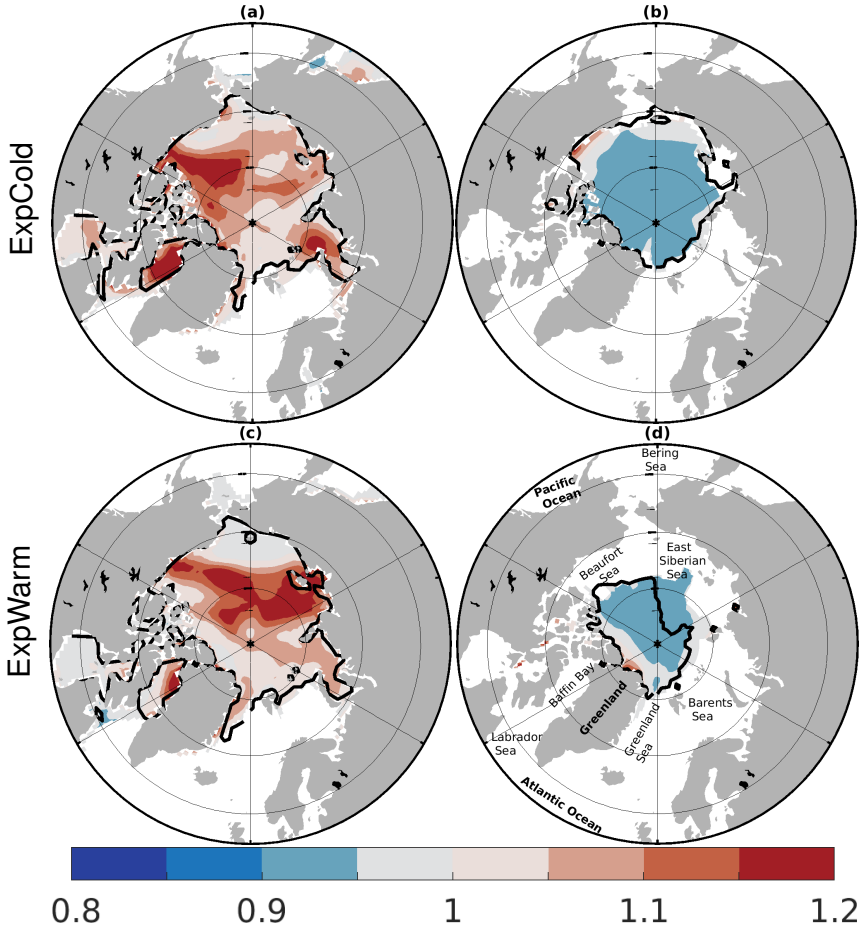

Figure S1. Factor modulated to turbulent heat fluxes over Arctic sea ice (SIC>70 %): (a) Late winter and (b) later summer for ExpCold. (c) and (d) as (a) and (b), but for ExpWarm. The regions with sea ice thickness $>$ 1 m in the PIOMAS reanalysis are compassed by black thick lines. Note: color only for the regions with SIC>70 %, while white areas indicating a constant factor of 1 (i.e. SIC $\leq$ 70 %).

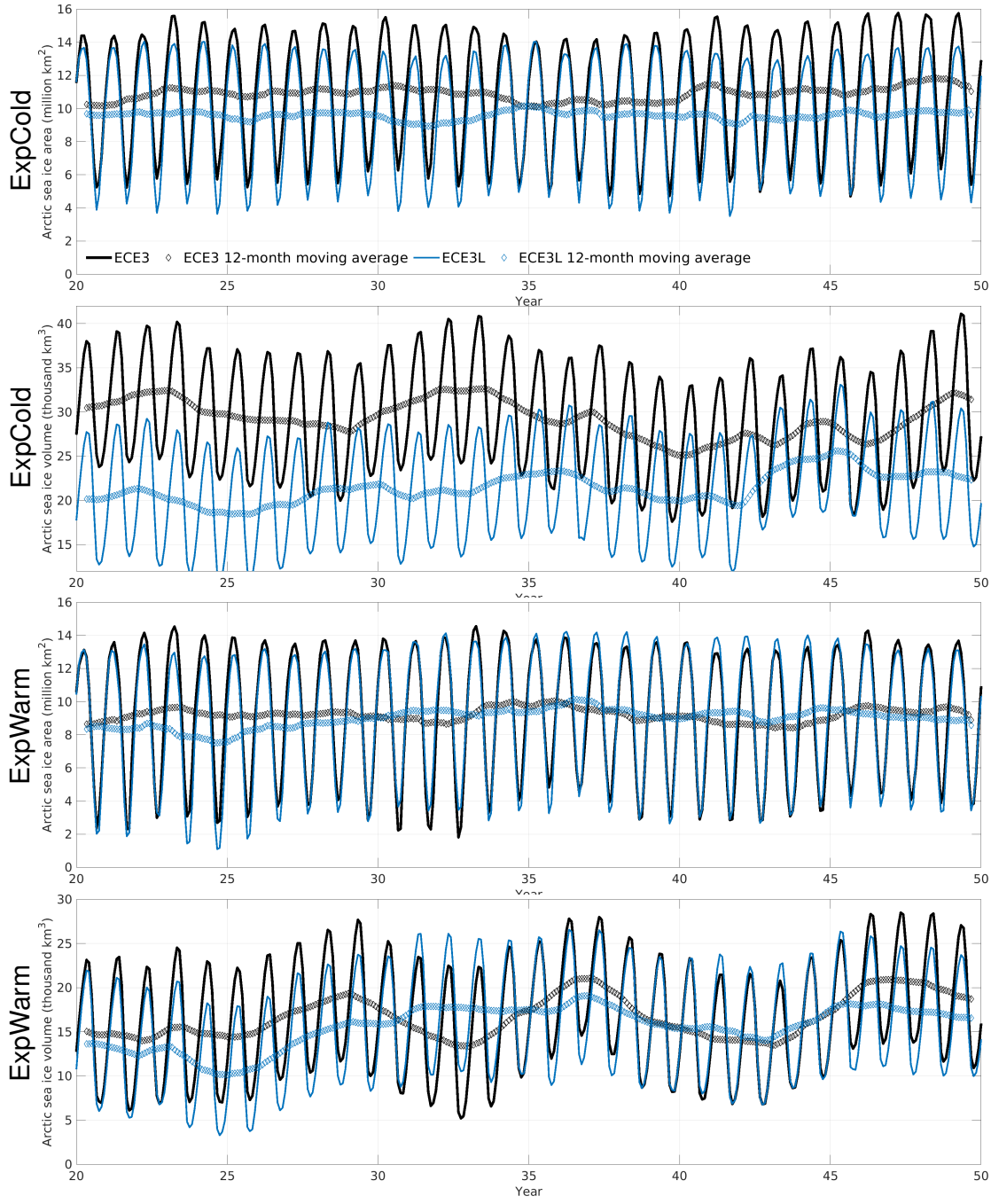

Figure S2. Seasonal cycle in ECE3 and ECE3L over the Arctic under a constant forcing: (a) Sea ice area and (b) Sea ice volume. Symbols represent the 12-month moving averages of the monthly values. The simulations are performed with the initial states and forcing for ExpCold. (c) and (d) as in (a) and (b), but for ExpWarm.

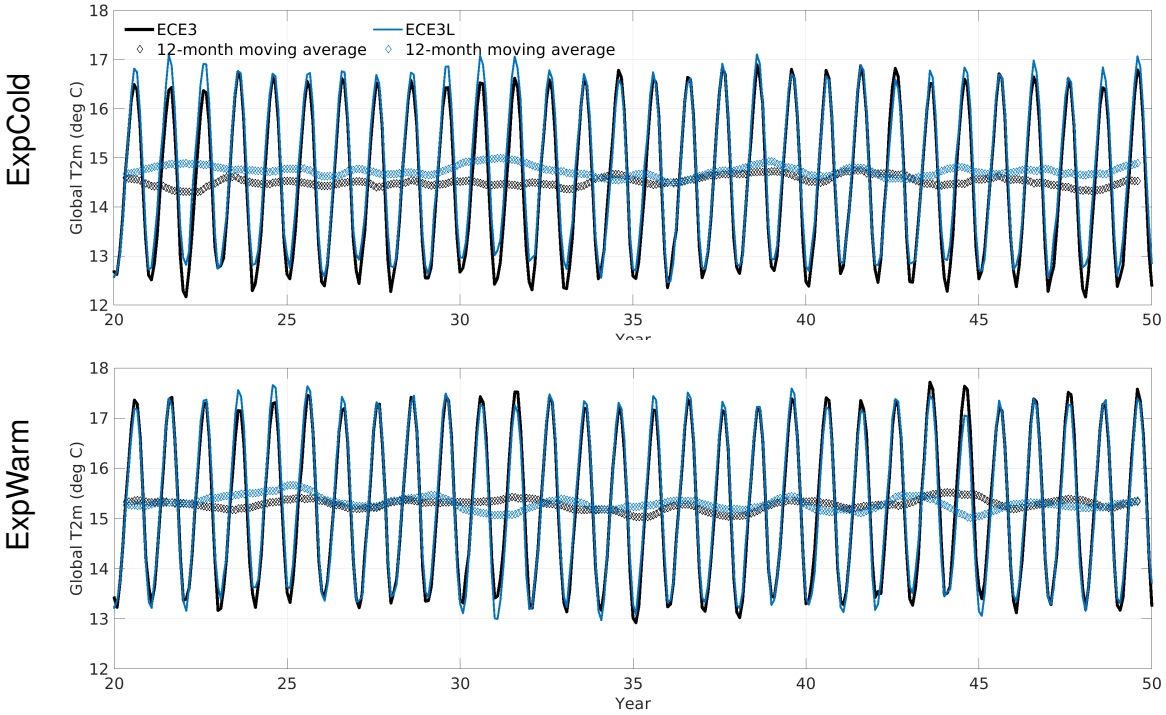

Figure S3. Time series of global surface air temperature at 2m (deg C) in ECE3 and ECE3L under a constant forcing: (a) ExpCold and (b) ExpWarm. Symbols represent the 12-month moving averages of the monthly values. The simulations are performed with the initial states and forcing for the respective years.

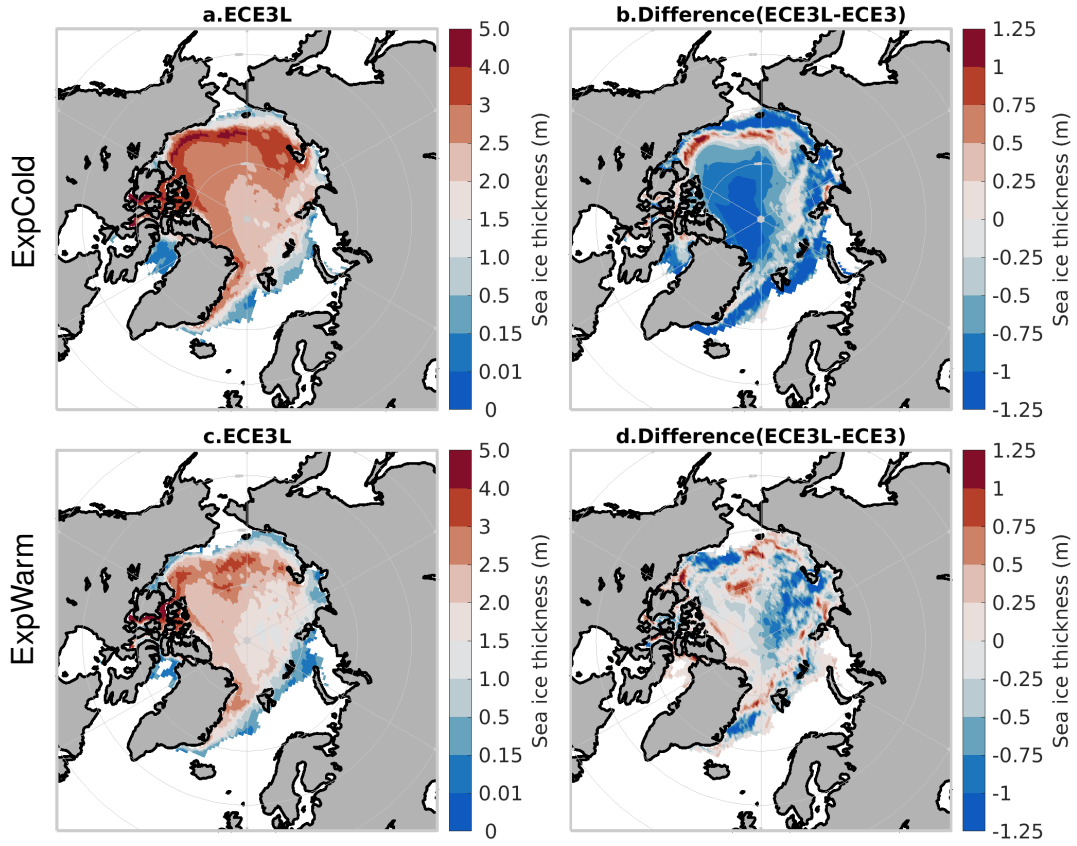

Figure S4. Late summer (September) Arctic sea ice thickness under a constant: for ExpCold (a) ECE3L, (b) Difference (ECE3L-ECE3). (c) and (d) as in (a) and (b), but for ExpWarm. Values are shown as 30 year averages as in Fig. **??**. Note: nonlinear color scale is used to emphasize thin ice categories. Thickness under 0.01 m is not shown.

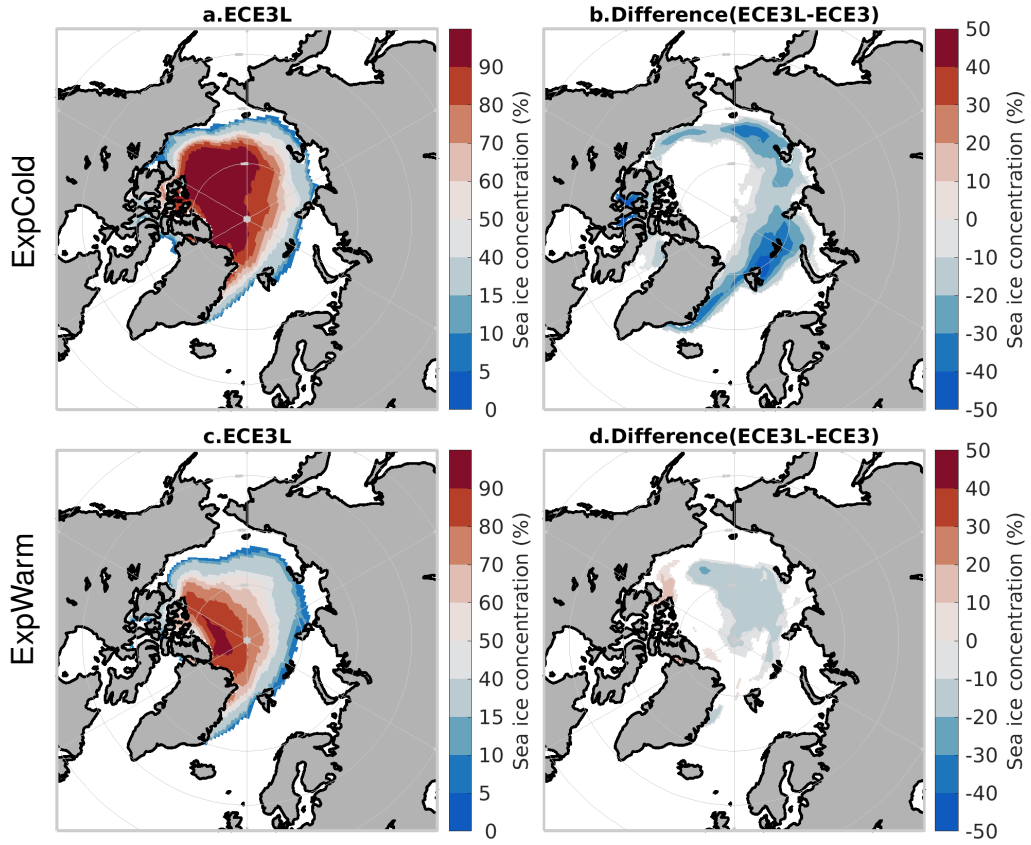

Figure S5. Late summer (September) Arctic sea ice concentration under a constant: for ExpCold (a) ECE3L, (b) Difference (ECE3L-ECE3). (c) and (d) as in (a) and (b), but for ExpWarm. Values are shown as 30 year averages as in Fig. **??**. Note: nonlinear color scale is used to emphasize low ice concentration. Concentration under 5 % is not shown.

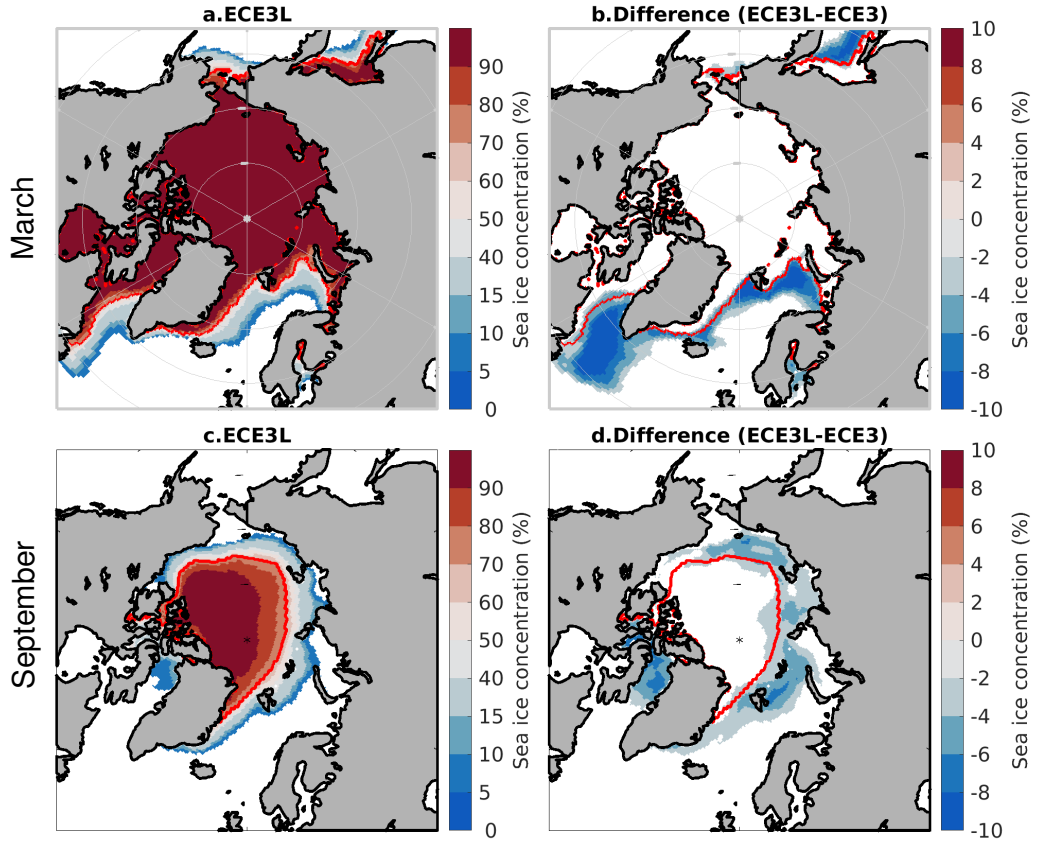

Figure S6. Ensemble mean Arctic maps (1980–2014): (a) ECE3L March sea ice concentration and (b) ECEL minus ECE3 difference. (c) and (d) as in (a) and (b), but for September. Note: nonlinear color scale is used to emphasize low ice concentration. Concentration under 5 % is not shown. The areas with SIC$\geq$70% in ECE3L is compassed by red lines.

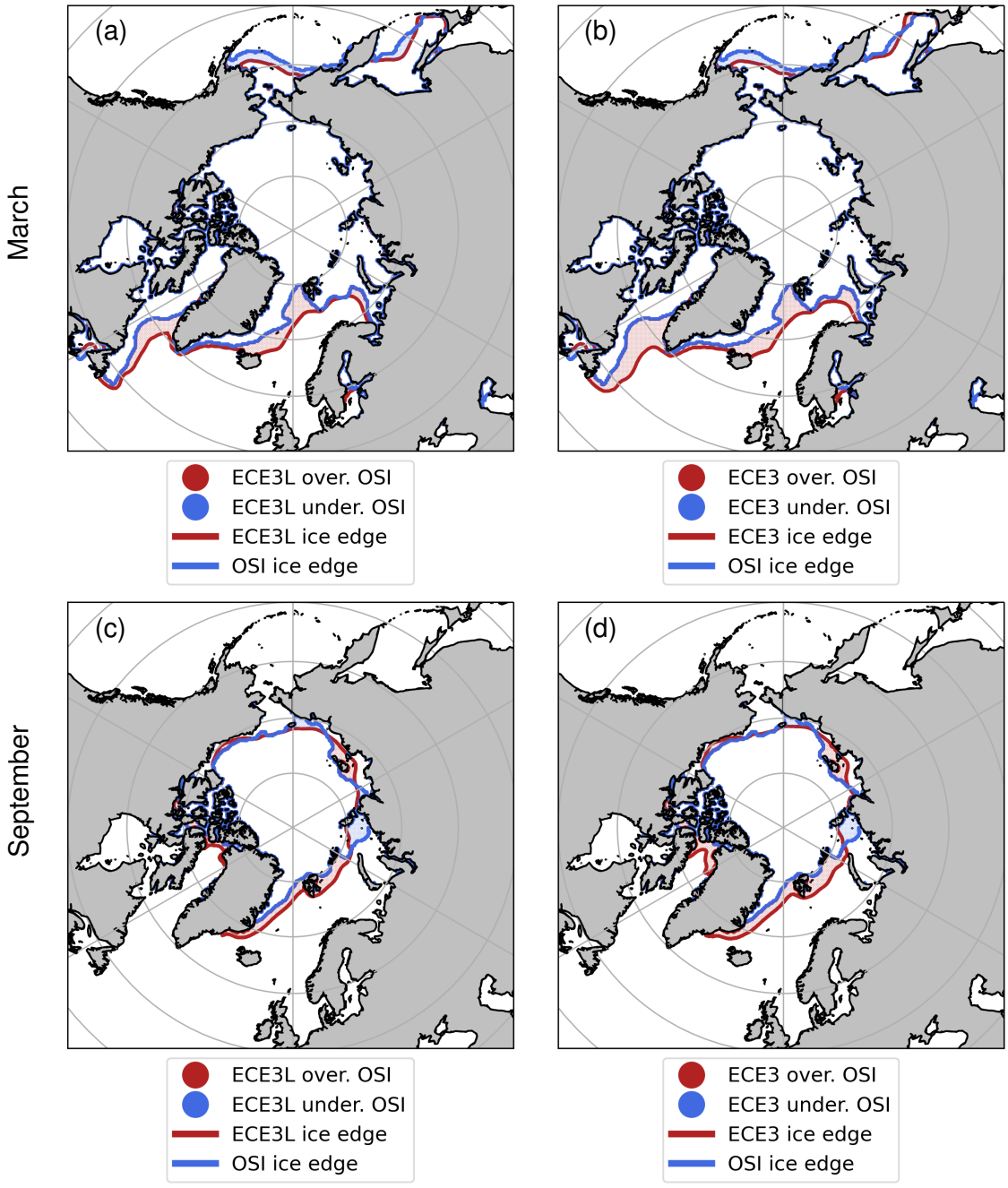

Figure S7. Integrated Ice Edge Error (IIEE, defined in section 2.3) maps of ECE3L (a)/ECE3 (b) ensemble mean vs. OSI-450a for March sea ice climatology (1980-2014). Red and blue indicate whether models overestimates or underestimates the ice edge prescribed by NSIDC-0051, respectively. (c) and (d) as in (a) and (b), but for September sea ice. Sea ice edge is defined by the 15%-sea ice concentration contour.

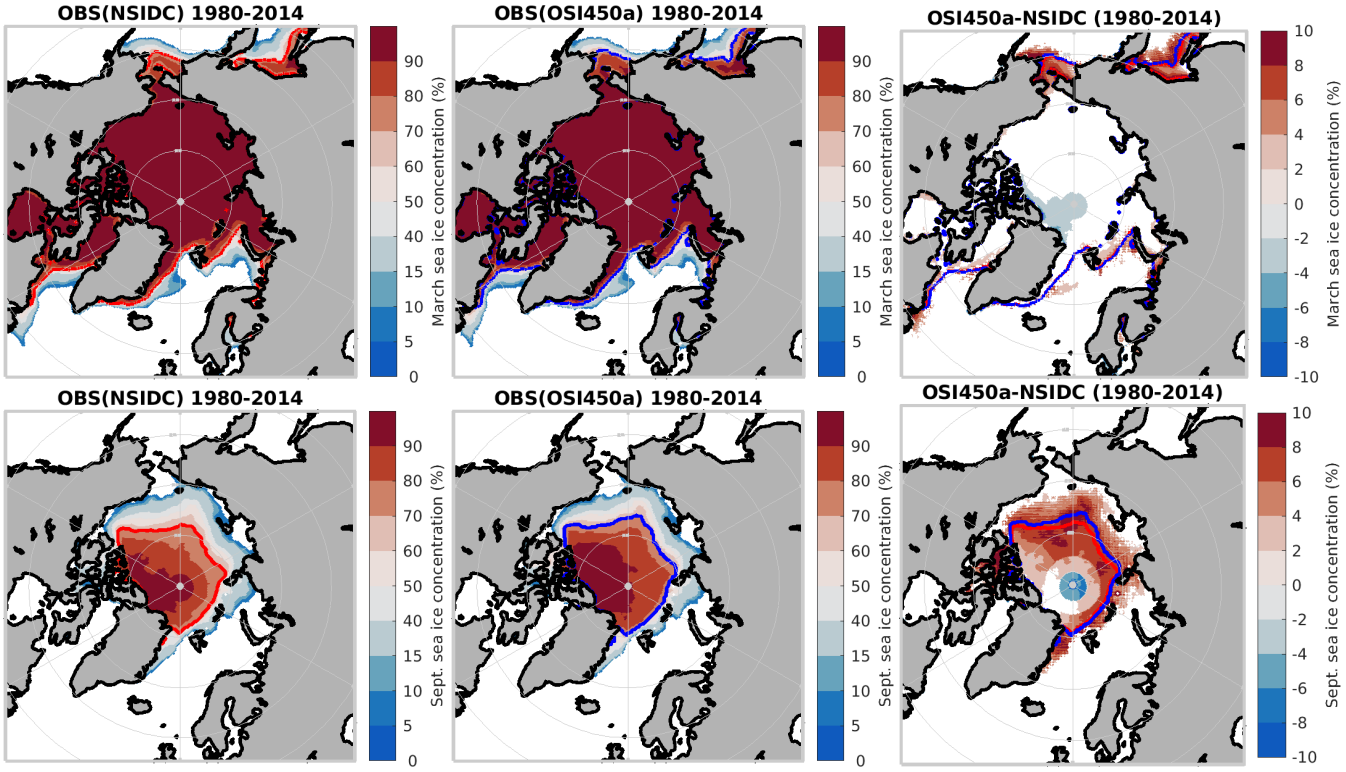

Figure S8. Satellite-derived Arctic sea ice maps (1980–2014): (a) NSIDC-0051 March concentration, (b) as in (a) but for OSI-450a, (c) OSI-450a minus NSIDC difference. Note: nonlinear color scale used to emphasize thin ice categories. (d,e,f) as (a,b,c) but for Sept. concentration. The areas with SIC$\geq$70% are compassed by red and blue lines for NSIDC and OSI-450a, respectively.

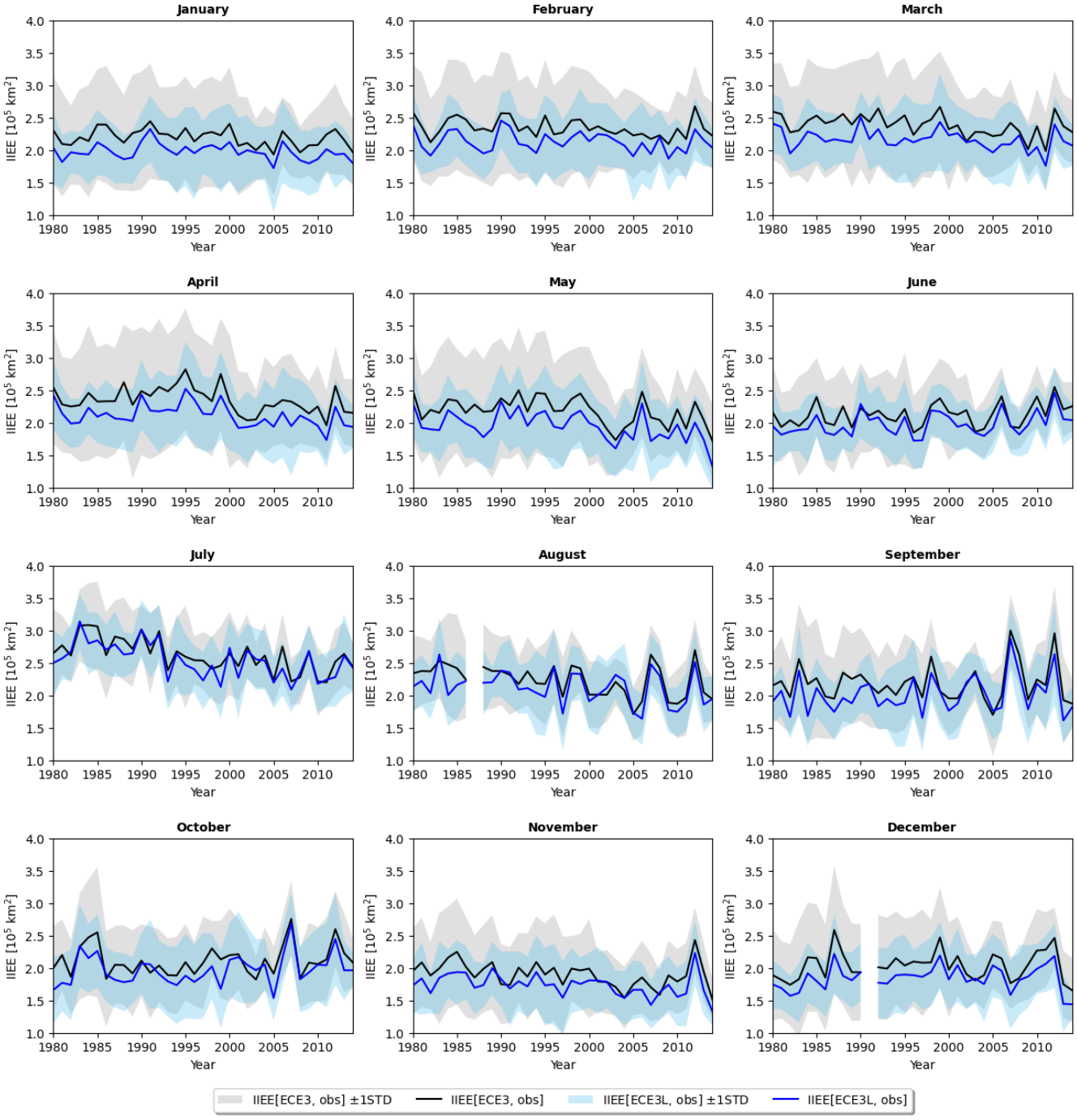

Figure S9. Time evolution of IIEE estimated for ECE3 (black) and ECE3L (blue) relative to NSIDC-0051 for each month (1980-2014) with the ensemble mean (in thick line) and model spread (shaded area) across 20 members calculated as one standard deviation from the mean. Sea ice edge is defined by the 15%-sea ice concentration contour.

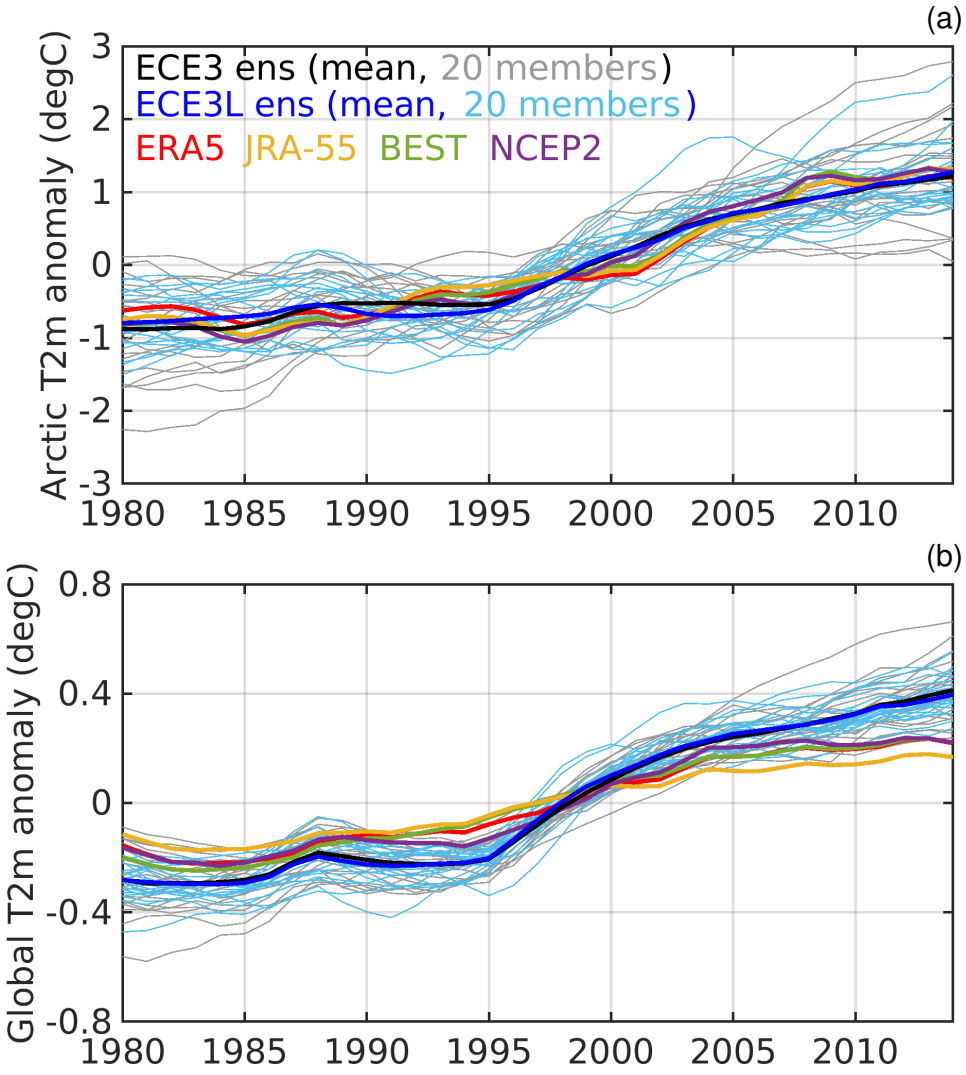

Figure S10. Annual mean temperature evolution for ECE3 and ECE3L from 1980 to 2014: (a) anomaly in the Arctic (66.5°–90°N), (b) as in (a) but for global annual mean. Observations are from ERA5 (Hersbach et al., 2020), Berkeley Earth (BEST, Rohde and Hausfather, 2020), JRA-55 (Kobayashi et al., 2015) and NCEP2 (Kanamitsu et al., 2002).